AIP Applied Physics Letters

Unusual photoresponse of indium doped ZnO/organic thin film heterojunction

Sesha Vempati, Saraswathi Chirakkara, J. Mitra, Paul Dawson, Karuna Kar Nanda et al.

Citation: Appl. Phys. Lett. **100**, 162104 (2012); doi: 10.1063/1.4704655
View online: http://dx.doi.org/10.1063/1.4704655
View Table of Contents: http://apl.aip.org/resource/1/APPLAB/v100/i16
Published by the AIP Publishing LLC.

Additional information on Appl. Phys. Lett.

Journal Homepage: http://apl.aip.org/
Journal Information: http://apl.aip.org/about/about_the_journal
Top downloads: http://apl.aip.org/features/most_downloaded
Information for Authors: http://apl.aip.org/authors

ADVERTISEMENT

Downloaded 21 Sep 2013 to 117.239.72.50. This article is copyrighted as indicated in the abstract. Reuse of AIP content is subject to the terms at: http://apl.aip.org/about/rights_and_permissions

Unusual photoresponse of indium doped ZnO/organic thin film heterojunction

Sesha Vempati,[1,a)] Saraswathi Chirakkara,[2] J. Mitra,[1,3,a)] Paul Dawson,[1] Karuna Kar Nanda,[2] and S. B. Krupanidhi[2]
[1]*Center for Nanostructured Media, School of Mathematics and Physics, Queen's University Belfast, County Antrim BT7 1NN, United Kingdom*
[2]*Materials Research Center, Indian Institute of Science, Bangalore 560 012, India*
[3]*School of Physics, Indian Institute of Science Education and Research, Thiruvananthapuram 695 016, India*

(Received 22 July 2011; accepted 31 March 2012; published online 17 April 2012; corrected 19 April 2012)

Photoresponse of *n*-type indium-doped ZnO and a *p*-type polymer (PEDOT:PSS) heterojunction devices are studied, juxtaposed with the photoluminescence of the In-ZnO samples. In addition to the expected photoresponse in the ultraviolet, the heterojunctions exhibit significant photoresponse to the visible (532 nm). However, neither the doped ZnO nor PEDOT:PSS individually show any photoresponse to visible light. The sub-bandgap photoresponse of the heterojunction originates from visible photon mediated *e-h* generation between the In-ZnO valence band and localized states lying within the band gap. Though increased doping of In-ZnO has limited effect on the photoluminescence, it significantly diminishes the photoresponse. The study indicates that optimally doped devices are promising for the detection of wavelengths in selected windows in the visible. © *2012 American Institute of Physics*. [http://dx.doi.org/10.1063/1.4704655]

ZnO-based inorganic/organic hybrid heterostructures comprise a topical case in point where many studies have addressed UV detection and photovoltaic applications.[1–6] While bare ZnO in various forms has been shown to the detect UV (Refs. 7 and 8) as well as white light,[9] heterojunctions offer significant advantages in terms of the wavelength selectivity and an improved response time of detection. Recent studies on *n*-Si/ZnO (Ref. 2) and *n*-ZnO/*p*-Si (Ref. 5) hybrid structures have shown bias polarity dependent UV and visible light detection and those on *n*-Si/*p*-ZnO (Ref. 6) junctions showed sensitivity without applied bias. In all cases, the final device sensitivity and selectivity are strongly influenced by the properties of the non ZnO component, i.e., the *p*-type component for an *n*-type ZnO sample. Poly(3,4-ethylenedioxythiophene):poly (styrenesulfonate) (PEDOT:PSS) is one such *p*-type conducting polymer with great potential in organic electronics.[10–12] Pioneering studies have already shown the possibilities of ZnO/PEDOT:PSS hybrid structures in opto-electronic applications, especially as light emitting diodes[12–16] and UV detectors;[17] low temperature fabrication capability being an added attraction. In this letter, we report on the fabrication and the photoresponse (PR) of *n*-type In doped ZnO (IZO) and PEDOT:PSS thin film heterojunctions. In addition to the expected UV PR,[17] corresponding to ZnO interband excitations, the heterojunctions exhibit significant PR to sub band gap excitation (to visible light at 532 nm). While the heterojunctions are UV active and visible blind under forward bias (FB); under reverse bias (RB), they have shown selective response to both the UV and visible. Interestingly, the present study also shows that neither bare IZO nor PEDOT:PSS individually exhibit any detectable PR to the visible but combined, the hybrid structure becomes visible sensitive. The PR to the visible is discussed with reference to the photoluminescence (PL) of the *n*-type IZO; specifically, the green emission band (500-600 nm) that is attributed to radiative recombination processes between ionized oxygen vacancy states[18–22] and the valence band (VB). Our results would suggest that the inverse process, where visible photons excite VB electrons to the localized intermediate states is responsible for the observed PR. The selective increase in the VB hole density (the excited electrons being localized in the vacancy states) in conjunction with the absence of PR in bare IZO suggest that the *p-n* junction is essential to elicit a strong visible PR from IZO. Notably, in contrast to previous reports of visible wavelength detection, with doped ZnO heterojunctions, the visible PR reported here originates from absorption and *e-h* generation in the ZnO itself rather than in the accompanying *p* or *n*-type component.[2,5,6] The PR and its dependence on doping concentration is further discussed in the context of an optimally doped ZnO/PEDOT:PSS visible detector.

100 nm thick films of In doped (1% and 3% by weight) ZnO were deposited on SiO_2/Si substrates by pulsed laser deposition with an O_2 partial pressure of 100 mTorr and 400 °C substrate temperature. As-deposited films were characterized by x-ray diffraction (XRD) (Bruker D8) and atomic force microscopy (Veeco Dimension). A 337.5 nm N_2 laser (Stanford Research Systems NL100) was used for excitation to record the PL spectra via a spectrograph fitted with a CCD camera (Acton Spectra Pro-275). The samples were further processed to fabricate multiple heterojunction devices; results from two such devices, D1 (1% doped) and D2 (3% doped), are presented here. Nominally ohmic contacts to the IZO were obtained by thermal evaporation of Al through a shadow mask. *p*-type PEDOT:PSS (Sigma Aldrich) was then spin coated onto the rest of the exposed IZO film to form the heterojunctions (Fig. 1(d)). Electrical contacts attached to

[a)]Authors to whom correspondence should be addressed. Electronic addresses: svempati01@qub.ac.uk and j.mitra@iisertvm.ac.in.

 © 2012 American Institute of Physics

Downloaded 21 Sep 2013 to 117.239.72.50. This article is copyrighted as indicated in the abstract. Reuse of AIP content is subject to the terms at: http://apl.aip.org/about/rights_and_permissions

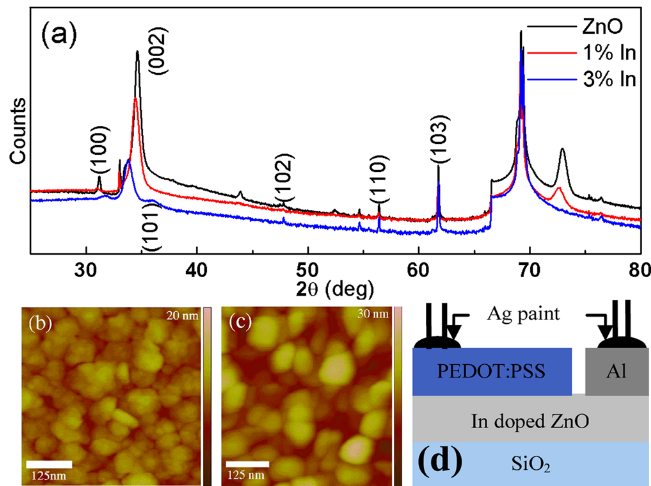

FIG. 1. (a) XRD on bare ZnO and 1% and 3% IZO films. AFM topography of (b) 1% and (c) 3% IZO films. (d) Schematic of the heterojunction devices.

the Al pad and to the polymer with Ag paint were used for current voltage (*IV*) measurements, conducted by sourcing a constant current and measuring the voltage in the four probe configuration. The *IV*s were collected upon excitation with two wavelengths $\lambda_1 = 360$ nm (3.4 eV), 60 mW from a Xe arc lamp with bandpass filter of width 10 nm and $\lambda_2 = 532.5$ nm (2.3 eV), 35 mW from a laser.

Analysis of the XRD patterns for the as-grown IZO films (Fig. 1(a)) shows preferentially (002) orientated growth perpendicular to the substrate,[23,24] exhibiting the characteristic wurtzite structure and well matched lattice parameters for ZnO. Grain size calculation estimates 34 nm and 20 nm grains for 1% and 3% doped IZO, respectively. Atomic force microscope images (Figs. 1(b) and 1(c)) indicate that SiO_2-IZO lattice mismatch leads to 3D island growth, with an average grain size of 40 nm and 25 nm for 1% and 3% IZO, respectively.

Figure 2 shows the room temperature PL spectra from the bare IZO films. The ZnO interband transition is evident at 390 nm (~3.2 eV) for both samples, along with a broad green emission. Spectral decomposition of the green emission of both samples reveals two components C_1 and C_2 centered at 527 nm (2.35 eV) and 570 nm (2.17 eV). The notable difference between the samples is the relative strength of C_1 and C_2, the ratios of which are 1.1 and 1.6 for the 1% and 3% IZO, respectively. As discussed in the literature, the origin of C_1 and C_2 emissions are ascribed to singly (V_O^+) and doubly (V_O^{++}) ionized oxygen vacancy states in ZnO,[18–22] with their relative strengths reflecting the relative abundance of the two ionization states.

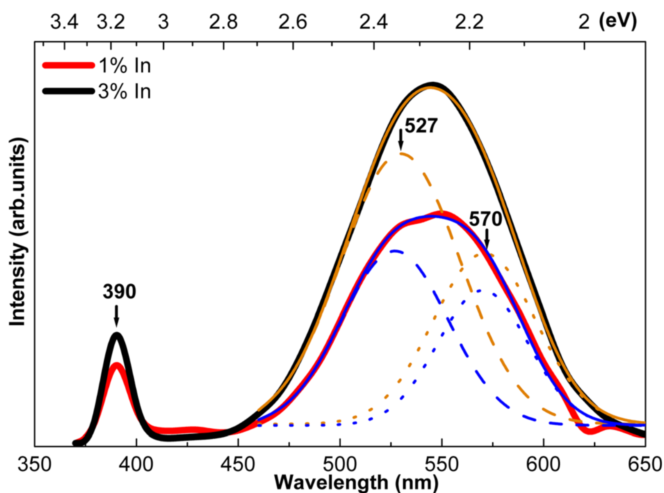

FIG. 2. Photoluminescence of the 1% and 3% indium doped ZnO films. Components C_1 (527 nm) and C_2 (570 nm) and envelopes are shown for both.

Figure 3(a) shows a schematic of the suggested emission[18,21] processes leading to the green components in the PL spectra. Within the bulk of the grains, the oxygen vacancies exist in the V_O^+ state; however band bending induced at the grain boundaries creates an electron deficient depletion region and the V_O^+ states therein are converted to V_O^{++} states by capturing surface trapped holes.[19–22] As observed by Ye *et al.*,[21] a strong correlation exists between the relative strength of C_1 and C_2 and their depletion region volume fraction, decided primarily by carrier concentration and grain size. The depletion width being inversely proportional to donor density (carrier density)[21] indicates that a higher carrier density results in a thinner depletion region, thus a smaller fraction of V_O^{++} states. Consequently, the higher doped and more conducting 3% film exhibits a weaker C_2 component as compared to the lower doped and less conducting 1% IZO (the conductance of the two films are evidenced in Figure 1, supplementary material[30]).

IV characteristics for devices D1 and D2 (Fig. 3(c)) were recorded under dark conditions and under illumination

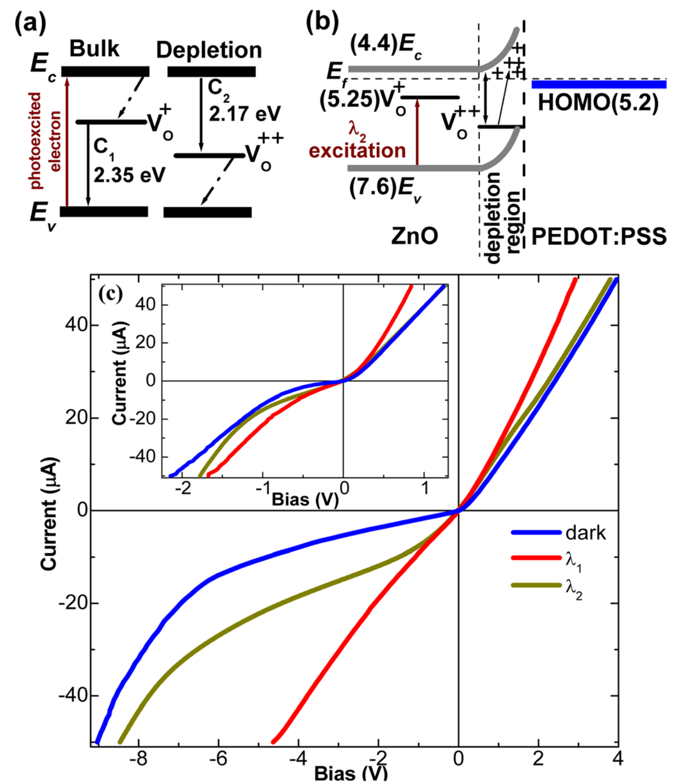

FIG. 3. (a) ZnO band diagram depicting origin of C_1 and C_2 emissions; dashed/solid arrows indicate non-radiative/radiative processes. E_c: conduction band, E_v: valence band, E_F: Fermi level. (b) Unbiased band structure of IZO/PEDOT:PSS heterojunction (Refs. 26 and 27) also showing photo excitation with λ_2. (c) *IV* spectra for 1% IZO/PEDOT:PSS heterojunctions in dark and with $\lambda_1 = 360$ nm and $\lambda_2 = 532$ nm illumination. Inset shows *IV* spectra for the 3% device.

Downloaded 21 Sep 2013 to 117.239.72.50. This article is copyrighted as indicated in the abstract. Reuse of AIP content is subject to the terms at: http://apl.aip.org/about/rights_and_permissions

at $\lambda_1 = 360$ nm (also see Figure 2 supplementary material[30]) and $\lambda_2 = 532$ nm. Note, the visible excitation λ_2 at 532 nm (2.33 eV) was specifically chosen to close to the peak energy of the C1 component of the PL spectra, reflecting the energy difference between the valence band edge and V_O^+ state in IZO. The FB dark *IVs* were fitted using the standard Richardson diode equation to calculate the saturation current density (J_s), ideality factor (n), and a junction barrier activation energy (ϕ). Values obtained for D1 were $J_s \sim 1.3 \times 10^{-5}$ A/cm^2, $n \sim 2.9$, and $\phi \sim 610$ meV. While the value of ϕ is comparable to existing reports of similar devices,[4,25] the value of n indicates that the device is closer to ideal than earlier reports. For D1, the λ_1 illuminated *IV* characteristics show an increase in junction conductivity for both bias polarities, though the increase in RB is significantly larger than that for FB. For $|V| > 1$ V in RB, more than 400% increase in current is observed, in contrast to typically 30% increase for FB. With λ_2 illumination under FB, D1 shows negligible PR. However, at -1 V RB $\sim$300% increase in current is detected, a response comparable to the UV (λ_1) PR seen earlier. The response weakens beyond -1 V. The 3% IZO device, D2 exhibits enhanced conductivity compared to D1, reflected in the higher currents observed for similar voltages (Fig. 3(c), inset). The calculated barrier activation energy and ideality factor from the dark *IV* are 675 meV and 2.0, respectively. As for D1, D2 is visible-blind under FB but retains a UV response. The RB PR, for D2, at λ_1 and λ_2 excitation is highly diminished though detectable.

The observed PR (*IVs*) can be explained on the basis of the suggested band diagram of IZO/PEDOT:PSS heterojunction (Fig. 3(b)).[18,21] The heterojunction consists of a *n*-type component with 3.2 eV band gap (ZnO valence and conduction band edges at 7.6 and 4.4 eV, respectively[26,27]) and the *p*-type component with the PEDOT HOMO at 5.2 eV.[14] Upon formation of the heterojunction, band bending within the positively charged depletion region created in IZO (Refs. 4 and 17) leads to accommodation of discontinuities in the conduction and valence band edges (at the interface) as band offsets ΔE_C and ΔE_V, respectively.[28] In the context of IZO, the above would also be accompanied by conversion of V_O^+ to V_O^{++} states, therein.[20] Under FB, the barrier potential gradient diminishes allowing thermally excited electrons in IZO and holes in PEDOT:PSS to cross the barrier and generate current. The majority electron current would be adversely affected by the presence of the added barrier ΔE_C. Similarly, the hole current would encounter a 2.4 eV barrier for hole injection from the PEDOT HOMO to the ZnO valence band edge.[14] When illuminated with λ_1, *e-h* pairs are selectively created in the IZO conduction and valence band, resulting in higher carrier density generating photo current.

Our investigations show that PEDOT:PSS shows no PR to either λ_1 or λ_2 illumination. Interestingly, bare IZO (contacted with Al electrodes) shows PR to λ_1 excitation but *none* for λ_2. (See Figs. 1 and 3 in supplementary material[30]). This symmetric Al-IZO-Al device comprises two back to back Schottky junctions, with one junction in FB the other in RB. Upon λ_2 illumination, electrons are excited from the IZO valence band to the intermediate vacancy states (V_O^+), the former hosting the holes. These carriers then must drift in opposite directions, towards the junctions (Al contacts) in order to contribute to the current. The excited electrons, confined to the narrow intermediate band with negligible mobility, would contribute little to the overall current. Schottky junctions are primarily majority carrier devices in sharp contrast to a *p-n* junction.[28] Hole conduction in a *n*-type semiconductor-metal Schottky junction is restricted to recombination processes with electrons, especially those from the conduction band (either excited or injected from the metal) and is masked by the dominant electron thermionic emission and tunneling channels. Since the λ_2 excitation does not alter the conduction band electron population in IZO, the overall current is negligibly affected by the VB hole generation. The low hole mobility (10 cm^2/Vs), small diffusion length (50 nm), and small life time[29] (10-50 ns) further compromises the hole conduction contribution. Consequently, bare IZO (Al-ZnO-Al) shows no detectable PR under λ_2 illumination. When the IZO/PEDOT:PSS heterojunctions are exposed to λ_2 excitation under FB, holes are again generated in the IZO VB with the electrons excited to the oxygen vacancy state. Here though a small PR is detected (Figure 3(c)), because the minority carrier current plays a more significant role in electrical transport across *p-n* junctions (i.e., larger contribution to the total current) as compared to its Schottky counterpart.

For the heterojunction devices under RB, the depletion width increases with increasing bias, accompanied by an increasing fraction of V_O^{++} states. The minority carrier density, i.e., holes in IZO, responsible for conduction under RB increases significantly with both λ_1 and λ_2 illumination. Owing to the strong electric field within the depletion region, photo generated *e-h* pairs therein are strongly pulled apart making them the primary contributors to the photo current. Consequently, PR increases monotonically with increasing RB. For λ_2 illumination, not only is the VB hole density increased additionally, the lifetime of these carriers are longer[19,29] compared to *e-h* pairs created by λ_1 excitation; thus benefiting the conduction process and increasing PR.

The study also shows that the devices have negligible PR in the wavelength window 400-500 nm. Further, in RB, the device D1 shows a larger PR compared to D2, the latter harboring the higher doped and more conducting IZO. The increased doping results in a higher free carrier concentration and would imply a thinner depletion region at the *p-n* junction adversely affecting the quantum efficiency[28] of the device leading to a lower PR.

To conclude, the laser ablated IZO films depicted good crystallanity and surface morphology with the photoluminescence spectra indicating the presence of localized intermediate states within the ZnO band gap, identified with singly and doubly ionized oxygen vacancy states. The presence of the intermediate states was harnessed to fabricate a visible range photo detector by creating an optimally doped PEDOT:PSS/IZO (1%) *p-n* junction that responds to visible range excitation at 532 nm, matching the energy gap between the valence band and intermediate states. The PR of the device was quantified by measuring their *IV* characteristics, which shows a significant PR with visible excitation that is comparable to the UV photoresponse. In contrast to previous reports of visible detection with ZnO heterojunctions, the photoresponse in the visible is elicited from *e-h* generation

Downloaded 21 Sep 2013 to 117.239.72.50. This article is copyrighted as indicated in the abstract. Reuse of AIP content is subject to the terms at: http://apl.aip.org/about/rights_and_permissions

in the ZnO rather than its counterpart. The heterojunction with 1% IZO depicted better PR compared with that of 3% doping. The resulting device shows selective PR for wavelengths below 400 nm and above 500 nm with negligible PR in between, displaying its potential as a wavelength selective detector.

The authors acknowledge the UK-India Education and Research Initiative for the financial support. S.V. acknowledges an international studentship from Queen's University Belfast.

[1]C. S. Lao, M. C. Park, Q. Kuang, Y. Deng, A. K. Sood, D. L. Polla, and Z. L. Wang, J. Am. Chem. Soc. **129**, 12096 (2007).
[2]Z. Guo, D. Zhao, Y. Liu, D. Shen, J. Zhang, and B. Li, Appl. Phys. Lett. **93**, 163501 (2008).
[3]Y.-Y. Lin, C.-W. Chen, W.-C. Yen, W.-F. Su, C.-H. Ku, and J.-J. Wu, Appl. Phys. Lett. **92**, 233301 (2008).
[4]S. Mridha and D. Basak, Appl. Phys. Lett. **92**, 142111 (2008).
[5]S. Mridha and D. Basak, J. Appl. Phys. **101**, 083102 (2007).
[6]H. Huang, G. Fang, X. Mo, L. Yuan, H. Zhou, M. Wang, H. Xiao, and X. Zhao, Appl. Phys. Lett. **94**, 063512 (2009).
[7]Z.-M. Liao, H.-Z. Zhang, and D.-P. Yu, Appl. Phys. Lett. **97**, 033113 (2010).
[8]H. Kind, H. Yan, B. Messer, M. Law, and P. Yang, Adv. Mater. **14**, 158 (2002).
[9]Y. Liu, Z. Zhang, H. Xu, L. Zhang, Z. Wang, W. Li, L. Ding, Y. Hu, M. Gao, Q. Li, and L. M. Peng, J. Phys. Chem. C **113**, 16796 (2009).
[10]D. Wakizaka, T. Fushimi, H. Ohkita, and S. Ito, Polymer **45**, 8561 (2004).
[11]E. Pal, T. Seemann, V. Zöllmer, M. Busse, and I. Dékány, Colloid. Polym. Sci. **287**, 481 (2009).
[12]T. Zhang, Z. Xu, D. L. Tao, F. Teng, F. S. Li, M. J. Zheng, and X. R. Xu, Nanotechnology **16**, 2861 (2005).
[13]C. S. Rout and C. N. R. Rao, Nanotechnology **19**, 285203 (2008).
[14]R. Könenkamp, R. C. Word, and M. Godinez, Nano Lett. **5**, 2005 (2005).
[15]A. Wadeasa, S. L. Beegum, S. Raja, O. Nur, and M. Willander, Appl. Phys. A: Mater. Sci. Process. **95**(3), 807 (2009).
[16]C. Y. Chang, F. C. Tsao, C. J. Pan, G. C. Chi, H. T. Wang, J. J. Chen, F. Ren, D. P. Norton, S. J. Pearton, K. H. Chen, and L. C. Chen, Appl. Phys. Lett. **88**, 173503 (2006).
[17]M. Nakano, T. Makino, A. Tsukazaki, K. Ueno, A. Ohtomo, T. Fukumura, H. Yuji, S. Akasaka, K. Tamura, K. Nakahara, T. Tanabe, A. Kamisawa, and M. Kawasaki, Appl. Phys. Lett. **93**, 123309 (2008).
[18]M. Ghosh and A. K. Raychaudhuri, Nanotechnology **19**(44), 445704 (2008).
[19]A. van Dijken, E. A. Meulenkamp, D. Vanmaekelbergh, and A. Meijerink, J. Phys. Chem. B **104**(8), 1715 (2000).
[20]K. Vanheusden, C. H. Seager, W. L. Warren, D. R. Tallant, and J. A. Voigt, Appl. Phys. Lett. **68**(3), 403 (1996).
[21]J. D. Ye, S. L. Gu, F. Qin, S. M. Zhu, S. M. Liu, X. Zhou, W. Liu, L. Q. Hu, R. Zhang, Y. Shi, and Y. D. Zheng, Appl. Phys. A: Mater. Sci. Process. **81**(4), 759 (2005).
[22]K. Vanheusden, W. L. Warren, C. H. Seager, D. R. Tallant, J. A. Voigt, and B. E. Gnade, J. Appl. Phys. **79**(10), 7983 (1996).
[23]S. B. Satish and I. S. Mulla, Sens. Actuators B **143**, 164 (2009).
[24]D. Craciun, G. Socol, N. Stefan, M. Miroiu, and V. Craciun, Thin Solid Films **518**, 4564 (2010).
[25]B. K. Sharma, N. Khare, and S. Ahmad, Solid State Commun. **149**, 771 (2009).
[26]L. Ley, R. A. Pollak, F. R. McFeely, S. P. Kowalczyk, and D. A. Shirley, Phys. Rev. B. **9**(2), 600 (1974).
[27]A. Hagfeldt and M. Gratzel, Chem. Rev. **95**, 49 (1995)
[28]S. M. Sze and K. K. Ng, *Physics of Semiconductor Devices*, 3rd ed (Wiley, New York, 2007).
[29]J. V. Foreman, J. Li, H. Peng, S. Choi, H. O. Everitt, and J. Liu, Nano Lett. **6**(6), 1126 (2006).
[30]See supplementary material at http://dx.doi.org/10.1063/1.4704655 for *IV*-characteristics of 1% and 3% In doped ZnO for dark, λ_1 and λ_2 illumination, dark and intensity variation with λ_1 in a semi-log plot for D1, and PEDOT:PSS for dark, λ_1 and λ_2 illumination.

Downloaded 21 Sep 2013 to 117.239.72.50. This article is copyrighted as indicated in the abstract. Reuse of AIP content is subject to the terms at: http://apl.aip.org/about/rights_and_permissions